RSC Advances

PAPER

Check for updates

Cite this: *RSC Adv.*, 2020, **10**, 24542

A LSER-based model to predict the solubilizing effect of drugs by inclusion with cucurbit[7]uril†

Enping Cheng,[a] Yangyan Zeng,[a] Yan Huang,[a] Tiezhu Su,[a] Yang Yang,[a] Li Peng*[a] and Jun Li *[abc]

A large number of traditional drugs and the development of new drugs often encounter the problem of poor water solubility. Cucurbit[7]uril, a novel macrocyclic host, has attracted great interest in this field. Investigating the solubilizing effect of drugs by inclusion with cucurbit[7]uril could provide guidance for drug solubilization. In this work, the interactions of drugs with cucurbit[7]uril, drugs with water and the inclusion complexes with water, and the properties of drugs and inclusion complexes, are considered to establish a linear solvation energy relationships (LSER)-based model. This model could be applied to predicting the solubility of drugs with cucurbit[7]uril in water. Density functional theory (DFT) is employed to obtain the properties and interaction parameters. The multi-parameter solubility model obtained by stepwise regression shows good fitting and predicting results. And the surface area of inclusion complexes (A_3), the LUMO energy of inclusion complexes (E_{3LUMO}), the polarity index of inclusion complexes (I_3), the electronegativity of drugs (χ_1), and the oil–water partition coefficient of drugs ($\log p_{1w}$) are effective parameters related to the solubilization of drugs with cucurbit[7]uril. Futhermore, the model could be extended to calculate the solubilizing effect of other macrocycles.

Received 16th April 2020
Accepted 18th June 2020

DOI: 10.1039/d0ra03394d

rsc.li/rsc-advances

1. Introduction

The challenge for the pharmaceutical industry is that about 40% of the top 200 drugs in the US are poorly soluble in water; and in the new chemical entity (NCE), the proportion of poorly water soluble drugs reached 90%.[1] Therefore, it is important to develop methods for improving their solubility. Now, many techniques have been employed to solve this problem, such as solid dispersion technology, synthetic prodrug technology, inclusion technology and so on. And the inclusion complexes technology could not only maintain the original properties and effects of drugs, but also improve their stability and bioavailability.[2] Although cyclodextrin is widely studied and used as a complexing agent,[3] it shows some shortcomings for practical application. For example, it would be easily hydrolyzed under acidic media, and the binding constant of cyclodextrin (including hydroxypropyl-β-cyclodextrin and sulfobutylether-β-cyclodextrin) is found to be lower than 10^5 M^{-1} in water.[4,5] Cucurbit[*n*]uril (n = 5–8, 10), another new macrocyclic host, shows good stability in both strong acid and weak alkaline solution.[6] In addition, cucurbit[*n*]uril exhibits much higher binding constant up to 10^{15} M^{-1} in water.[7] So cucurbit[*n*]uril has attracted widespread attention due to its high selectivity and affinity with guest.[8,9]

Cucurbit[*n*]uril (n = 5–8, 10), the symmetrical macrocyclic cage compounds, formed by a series of glycoluril through methylene linkage, have a hydrophilic portal and hydrophobic cavity. Compared with other cucurbit[*n*]uril host, cucurbit[7]uril has relatively high solubility in water (20–30 mM or 23–35 g L^{-1}).[10] Although the solubility of drugs by inclusion with cucurbit[7]uril could be confirmed through experiment to identify effective drug candidates,[11] it has certain limitations in terms of cost, time and resources. Instead of, theoretical prediction method could quickly and efficiently screen out drugs with good solubilizing effect by cucurbit[7]uril. However, there is few theoretical study on the solubilizing effect of cucurbit[7]uril on drugs, which hinders its extensive application in the pharmaceutical industry. As an alternative, it was reported that linear solvation energy relationships (LSER) could be used to calculate the solubility of various compounds in water.[12–14] But there was no LSER-based model for predicting the solubility of drugs with cucurbit[7]uril in water.

Therefore, the purpose of this study is to establish a suitable LSER-based model to predict the solubilizing effect of cucurbit[7]uril on drugs with poor water solubility. In line with this, the interactions of drugs with cucurbit[7]uril, drugs with water and the inclusion complexes with water, the properties of drugs and

[a]College of Chemistry and Chemical Engineering, Xiamen University, Xiamen 361005, China. E-mail: li.peng@xmu.edu.cn; junnyxm@xmu.edu.cn; Tel: +86-592-2183055

[b]Collaborative Innovation Center of Chemistry for Energy Materials, Xiamen 361005, China

[c]National Engineering Laboratory for Green Chemical Productions of Alcohols, Ethers and Esters, Xiamen 361005, China

† Electronic supplementary information (ESI) available: Detailed information for the experimental solubility data and optimized inclusion structures and parameters. See DOI: 10.1039/d0ra03394d

This article is licensed under a Creative Commons Attribution-NonCommercial 3.0 Unported Licence.

This journal is © The Royal Society of Chemistry 2020

inclusion complexes, are analysed for the LSER-based model establishment. Then DFT is applied for calculating all the parameters. On one hand, this model could quickly screen out drugs with good solubilizing effect by cucurbit[7]uril. On the other hand, the model would provide guidance for the modification of cucurbit[*n*]uril after clarifying the solubilizing mechanism.

2. Materials and methods

2.1 Experiment and data set

To obtain the experimental solubility data of drugs, excess drugs (VB_2, triamterene, guanine, 2-hydroxychalcone, gefitinib) were added to 10 mL of aqueous solutions containing various concentrations of cucurbit[7]uril (0–15.0 mM or 0–17.4 g L^{-1}). The samples were vibrated for 1 h on an ultrasonic equipment and then stirred at room temperature in dark until equilibrium was reached (24 h). Afterwards, samples were filtered and diluted with H_2O for UV-vis spectroscopic measurement. The ultraviolet absorption peaks (VB_2, at 446 nm; triamterene, at 358 nm; guanine, at 295 nm; 2-hydroxychalcone, at 323 nm; gefitinib, at 335 nm) were measured on a ThermoEvolution 220 spectrophotometer. The experimental solubility data of drugs with cucurbit[7]uril in water and logarithm of solubility are listed in Table 1. Note that the data for drugs signed with *a* was measured by UV-vis spectroscopy approach in this work which was shown in Fig. S1–S6.† The solubility data for the rest of drugs are collected from publications.

2.2 Establishment of LSER-based model

The original model of LSER describes the linear relationship between molecular property and the solubility of a solute–solvent system; it could be expressed by eqn (1):[29–32]

$$\log Y = c + x_1X_1 + x_2X_2 + x_3X_3 \quad (1)$$

where Y represents the physical and chemical properties of molecules, such as solubility, toxicity, activity; X_1, X_2, X_3 are the properties-related parameters; x_1, x_2, x_3 are the parameters-related coefficients; c is a constant. The LSER model reported in literature, studying the solubility of various molecules in water, could be described as follows:[33–38]

$$\log S = c + vD + eE + iL \quad (2)$$

where S is the solubility of molecules; D is the molecular dimension; E is the molecular interaction; L represents the macroscopic properties of molecules.

Generally, the solubility could be predicted by the solute–solvent intermolecular forces, but it was not sufficient to calculate the solubility of inclusion complexes. For the inclusion system in water, with respect to the main molecular parameters influencing the solubility could be divided into three categories as shown in Fig. 1. The first is the molecular interaction between the drugs and cucurbit[7]uril, where the interaction energy should be considered, involving the van der Waals' force, hydrogen bond and other forces. Cucurbit[7]uril

Table 1 Experimental solubility data of drugs by inclusion with cucurbit[7]uril in water

Drug	S/g L^{-1}	S/μM	log S/μM
Cinnarizine[15]	5.049	13 700.000	4.137
Allopurinol[16]	1.200	8816.000	3.945
MEABZ[17]	2.259	7300.000	3.863
Albendazole[1]	1.884	7100.000	3.851
Thiabendazole[18]	0.968	4810.000	3.682
6-Benzyladenine[19]	1.023	4540.000	3.657
Gefitinib[a]	1.734	3880.891	3.589
Kinetin[20]	0.820	3810.000	3.581
Nandrolone[11]	1.015	3700.000	3.568
Norharmane[21]	0.622	3700.000	3.568
Triamterene[a]	0.923	3643.070	3.561
2-Hydroxychalcone[a]	0.405	1807.433	3.257
Vitamin B_9 (VB_9)[a]	0.730	1654.000	3.219
Fuberidazole[22]	0.265	1440.000	3.158
10-Hydroxycamptothecine[23]	0.475	1303.000	3.115
Prednisolone[11]	0.458	1137.000	3.056
Clofazimine[24]	0.514	1085.000	3.035
β-Estradiol[11]	0.295	1083.000	3.035
Vitamin B_2 (VB_2)[a]	0.353	937.862	2.972
3-Cyano-6-(2-thienyl)-4-trifluoromethyl pyridine (TFP)[25]	0.249	924.000	2.966
Progesterone[11]	0.223	708.000	2.850
Cholic acid[11]	0.287	702.000	2.846
Cortisol[11]	0.246	680.000	2.833
TPP[26]	0.357	580.018	2.763
Guanine[a]	0.082	540.489	2.733
Estriol[11]	0.149	516.000	2.713
Estrone[11]	0.136	504.000	2.702
TPPZn[26]	0.306	451.377	2.655
Camptothecin[1]	0.139	400.000	2.602
Coumarin 6 (ref. 27)	0.131	375.000	2.574
Megestrol acetate[11]	0.137	369.000	2.567
Zaltoprofen[28]	0.076	254.000	2.405
Cholesterol[11]	0.017	45.000	1.653
Estradiol-3-benzoate[11]	0.014	36.000	1.556
17-Ethinyl estradiol[11]	0.009	30.000	1.477

[a] The data for drugs that was measured by UV-vis spectroscopy approach.

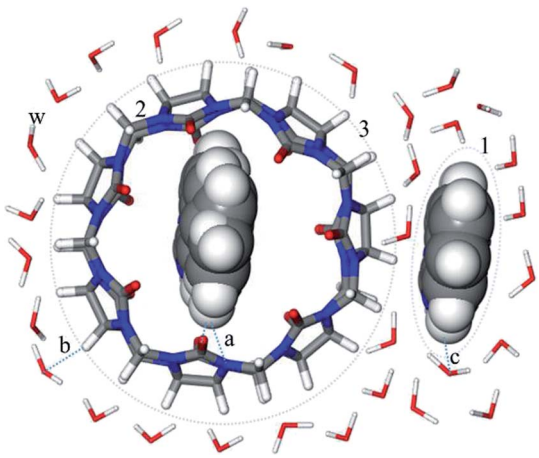

Fig. 1 Design of parameters related to the solubility of drugs in presence of cucurbit[7]uril ((a) interaction between the drugs and cucurbit[7]uril; (b) interaction between the inclusion complexes and water; (c) the drugs in water; 1: drugs; 2: cucurbit[7]uril; 3: inclusion complexes; w: water).

mainly bonds with various organic molecules through the hydrophobic interaction of the cavity and the hydrogen bonding of the carbonyl groups at both ends.[39] The second is the molecular interaction between inclusion complexes and water. For this the solvation energy is directly obtained instead of the van der Waals' force and hydrogen bond should be also considered.[40] The third is the interaction between drugs and water, where the oil–water partition coefficient of drugs directly indicates the dissolution of drugs in water.[33] Besides the main parameters mentioned above, the molecular dimensions are considered in model, such as the size of inclusion complexes and the drug size. Accordingly, we propose a LSER-based model for the drug–cucurbit[7]uril–water system:

$$\log S = c + d_1D_1 + d_3D_3 + e_{12}\Delta E_{12} + h_{12}H_{12} + e_{3w}\Delta G_{3w} + w_{3w}W_{3w} + h_{3w}H_{3w} + p_{1w}\log p_{1w} \quad (3)$$

where subscript 1 represents drugs; 2 represents cucurbit[7]uril; 3 represents the drug–cucurbit[7]uril inclusion complexes; 12 represents the interaction between drug and cucurbit[7]uril; 3w refers to the inclusion complexes in water. D_1 is the size of drugs; D_3 is the size of inclusion complexes; ΔE_{12} represents the interaction energy between drugs and cucurbit[7]uril; H_{12} indicates the hydrogen bond between drugs and cucurbit[7]uril; ΔG_{3w} is the solvation energy of inclusion complexes; W_{3w} represents the van der Waals' force between inclusion complexes and water; H_{3w} represents the hydrogen bond between inclusion complexes and water; $\log p_{1w}$ is the oil–water distribution coefficient of drugs. d_1, d_3, e_{12}, h_{12}, e_{3w}, w_{3w}, h_{3w}, p_{1w} are parameter-related coefficients; c is a constant.

The parameters in eqn (3) could be replaced by quantum chemical parameters as shown in eqn (4):

$$\log S = c + v_1V_1 + a_3A_3 + e_{12}\Delta E_{12} + x_1\chi_1 + e_{3w}\Delta G_{3w} + m_3I_3 + g_3E_{3LUMO} + p_{1w}\log p_{1w} \quad (4)$$

where the volume of drugs (V_1) is used to identify D_1 in eqn (3). The surface area of inclusion complexes (A_3) is applied to D_3 in eqn (3). H_{12} in eqn (3) is replaced by the electronegativity of drugs (χ_1). According to the HOMO/LUMO electron distribution diagram of inclusion complexes, it is known that LUMO is distributed on cucurbit[7]uril.[41,42] The LUMO energy of inclusion complexes (E_{3LUMO}) is applied to H_{3w} in eqn (3).[43] Generally, water is electron donor, and E_{3LUMO} is electron acceptor, so E_{3LUMO} describes the hydrogen bond between inclusion complexes and water. The polarity of inclusion complexes (I_3) is applied to W_{3w} in eqn (3).[44]

2.3 Calculation details

The chemical structures of all drug molecules are optimized using the Gaussian software (version 09, Gaussian, Inc., http://gaussian.com, USA), in which the B3LYP functional method is applicable to calculating molecular properties. The structures of the inclusion complexes of cucurbit[7]uril with various drugs are optimized at the B3LYP/6-311G* level. And frequency calculations are performed on the same level for all possible geometries to ensure they are minimal on the potential surface (Fig. S7†). Solvation effects were evaluated by employing the solvation model based on density (SMD).

The interaction energy between drugs and cucurbit[7]uril (ΔE_{12}) and the solvation energy of inclusion complexes (ΔG_{3w}) are calculated respectively by eqn (5) and (6):

$$\Delta E_{12} = E_3 - E_2 - E_1 + E_{BSSE} \quad (5)$$

$$\Delta G_{3w} = E_{3sol} - E_{3gas} \quad (6)$$

where E_3 represents the total energy of inclusion complexes; E_2 is the total energy of cucurbit[7]uril; E_1 is the total energy of drugs; E_{BSSE} represents the basic set superposition error; E_{3sol} represents the single-point energy of inclusion complex calculated in water; E_{3gas} represents the single-point energy of inclusion complex calculated under the gas phase. The single point energy is calculated at the M062X/6-311G* level. The electronegativity of drugs (χ_1) is calculated by eqn (7)–(9):

$$\chi_1 = \frac{IP + EA}{2} \quad (7)$$

$$IP = \frac{E(N-1) + E(N)}{2} \quad (8)$$

$$EA = \frac{E(N) + E(N+1)}{2} \quad (9)$$

where IP is the ionization energy and EA is the electron affinity, the single point energy is calculated using B3LYP/6-311G*, N is the number of electrons when electrically neutral.

The E_{3LUMO} parameter in eqn (4) is obtained from the optimized structure. The parameter of $\log p_{1w}$ is obtained from the Material Studio software (version 8.0, Accelrys Inc., http://www.accelrys.com, USA). The parameters I_3, A_3 and V_1 are obtained in combination with the Multiwfn software,[44] where the electron density is 0.001 a.u. (electrons per bohr^3) contour surface.

The fitting coefficient (R^2), leave-one-out cross-validation correlation coefficient ($Q_{LOO}{}^2$), F-test, t-test, inflation factor (VIF), and Durbin–Watson coefficient (DW) are employed to validate the LSER-based model by using the SPSS software (version 25.0, SPSS Inc., http://www.spss.com).[45] External test is applied to the prediction effect and application domain of the predication model, not used for building the LSER model. As reported,[46,47] when the predictive squared correlation coefficient ($Q_{F1}{}^2$, $Q_{F3}{}^2$) is greater than 0.600, and the concordance correlation coefficient (CCC) is greater than 0.850, it is a successful model for prediction.

$$Q_{F1}{}^2 = 1 - \frac{\sum_{i=1}^{n_{TE}} (\tilde{y}_i - y_i)^2}{\sum_{i=1}^{n_{TE}} (y_i - \bar{y}_{TR})^2} > 0.600 \quad (10)$$

$$Q_{F3}{}^2 = 1 - \frac{\sum_{i=1}^{n_{TE}} (\tilde{y}_i - y_i)^2 \Big/ n_{TE}}{\sum_{i=1}^{n_{TR}} (y_i - \bar{y}_{TR})^2 \Big/ n_{TR}} > 0.600 \quad (11)$$

 This journal is © The Royal Society of Chemistry 2020

$$\mathrm{CCC} = \frac{2\sum_{i=1}^{n_{\mathrm{TE}}}(y_i - \bar{y})(\tilde{y} - \bar{\tilde{y}})}{\sum_{i=1}^{n_{\mathrm{TE}}}(y_i - \bar{y})^2 + \sum_{i=1}^{n_{\mathrm{TE}}}(\tilde{y} - \bar{\tilde{y}})^2 + n_{\mathrm{TE}}(\tilde{y} - \bar{\tilde{y}})^2} > 0.850 \quad (12)$$

where y_i and $\tilde{y}_i$ are the experimental and calculated values, respectively; $\bar{y}_{\mathrm{TR}}$ is the average of the experimental values of the training set; $\bar{\tilde{y}}$ is the average of the calculated values; n_{TR} and n_{TE} are the numbers of samples in the training and test sets, respectively.

3. Results and discussion

3.1 Modelling results

From DFT, the parameters of drugs–cucurbit[7]uril inclusion complexes are shown in Table S1.† In this study, the solubility of drugs obtained from literature are applied as the training set to build the LSER model, and the solubility of drugs (7, 11, 12, 19, 25) experimentally measured in this work are used as the test set.

To select most informative parameters and exclude redundant ones, the multiple linear stepwise regression was employed with log S as the dependent variable (Table 1) and the quantum-chemical parameters (Table S1†) as the independent variables. The fitting coefficient (R^2) and the leave-one-out cross-validation correlation coefficient ($Q_{\mathrm{LOO}}{}^2$) are used to determine the optimum number of parameters for the LSER-based model. If both R^2 and $Q_{\mathrm{LOO}}{}^2$ are greater than 0.600,[45] at the same time with R^2–$Q_{\mathrm{LOO}}{}^2$ less than 0.300, this model would meet the criterion of "good model" proposed by Eriksson *et al.*[48] Fig. 2a showed the performance of the model is not significantly improved when the parameters exceed six (the order of 1–8 parameter selection is based on the parameter's contribution rate: A_3, $E_{3\mathrm{LUMO}}$, $\log p_{1\mathrm{w}}$, I_3, χ_1, ΔE_{12}, V_1, $\Delta G_{3\mathrm{w}}$). Five parameters are randomly selected for fitting. According to Fig. 2b, A_3, $E_{3\mathrm{LUMO}}$, $\log p_{1\mathrm{w}}$, I_3, χ_1 has the largest fitting coefficient.

Therefore, the five-parametric model (eqn (13)) is finally determined as the optimum LSER-based model after evaluating the fitting coefficient, cross-validation (Fig. 2), and correlation of the parameters (Table 4).

$$\log S = -16.452 + 22.859\left(\frac{A_3}{10000}\right) + 14.301\chi_1 + 20.347(10I_3) + 2.898(10E_{3\mathrm{LUMO}}) - 1.119\left(\frac{\log p_{1\mathrm{w}}}{10}\right) \quad (13)$$

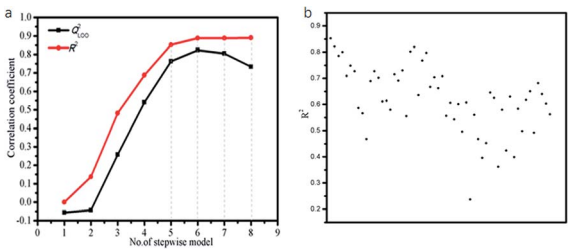

Fig. 2 (a) The plot of model performance *vs.* number of variables included in LSER model. (b) The plot of fitting coefficient *vs.* different five parameters included in LSER model.

Table 2 Various statistics parameters of the LSER-based model

m^a	$n_{\mathrm{TR}}{}^b$	$n_{\mathrm{TE}}{}^c$	R^{2d}	$\mathrm{RMSE_{TR}}{}^e$	$Q_{\mathrm{LOO}}{}^{2f}$
5	30	5	0.852	0.254	0.763

$\mathrm{RMSE_{cv}}{}^g$	F^h	DW^i	$Q_{\mathrm{F1}}{}^2$	$Q_{\mathrm{F3}}{}^2$	CCC
0.322	2.678	1.402	0.710	0.890	0.863

[a] Number of descriptors applied for the model development. [b] Number of molecules in training set. [c] Number of molecules in test set. [d] Training correlation coefficient. [e] Training root mean square error. [f] Leave-one-out cross-validation correlation coefficient. [g] Leave-one-out cross-validation root-mean-square errors. [h] *F*-Test. [i] Durbin–Watson coefficient.

Table 3 Standardized and unstandardized coefficients of the LSER-based model (eqn (13)), and their *t* and *p* values

#	Unstandardized coefficients	Standardized coefficients	*t*-Value	*p*-Value
c	−16.452	—	−7.659	0.000
χ_1	14.301	0.659	5.160	0.000
$\log p_{1\mathrm{w}}$	−1.119	−0.399	−3.296	0.003
A_3	22.859	1.513	10.003	0.000
$E_{3\mathrm{LUMO}}$	2.898	0.846	5.253	0.000
I_3	20.347	0.823	5.927	0.000

The five parameters includes the surface area of inclusion complexes (A_3), the electronegativity of drugs (χ_1), the polarity index of inclusion complexes (I_3), the LUMO energy of inclusion complexes ($E_{3\mathrm{LUMO}}$), the oil–water partition coefficient of drugs ($\log p_{1\mathrm{w}}$).

This model confirmed an acceptable relationship between the number (5) of variables and the number (30) of drugs, where the ratio of the number of variables to the number of drugs is greater than 5 : 1.[49] According to Table 2, the fitting coefficient (R^2) of the LSER-based model is 0.852, which is much larger than 0.600. And the root-mean-square error is 0.254, which is relatively small.

In order to determine whether there are "outliers" in the LSER-based model, a cross-validation method is used for testing. The high value of correlation coefficient of leave-one-out ($Q_{\mathrm{LOO}}{}^2 = 0.763$) and the acceptable value of cross validation root mean square error ($\mathrm{RMSE_{cv}} = 0.322$) prove the stability of the LSER-based model. In addition, R^2–$Q_{\mathrm{LOO}}{}^2$ is 0.089, less than 0.3, which meets the criterion of "good model". Therefore, it is further confirmed that the established LSER-based model is reliable.

Generally, $P < 0.050$ indicates that this parameter has an effect on the model. According to Table 3, it is known that the P value of each parameter is close to 0.000, indicating that these five parameters have a significant effect on the LSER-based model. The unstandardized coefficients in Table 3 are used to construct the equation. The standardized coefficient is

Table 4 Correlation coefficient between the parameters of LSER-based model (eqn (13)) and their VIF values

	χ_1	$\log p_{1w}$	A_3	E_{3LUMO}	I_3	VIF
χ_1	1	−0.364	−0.107	−0.485	−0.096	2.650
$\log p_{1w}$		1	0.670	−0.357	−0.569	2.381
A_3			1	−0.639	−0.767	3.714
E_{3LUMO}				1	0.708	4.209
I_3					1	3.130

Table 5 The calculated log S data obtained from eqn (13) and the relative error (RE)

#	log S/μM	RE
Progesterone	2.791	−2.057%
Nandrolone	3.259	−8.671%
Megestrol acetate	2.334	−9.096%
Cortisol	3.214	13.475%
Estrone	2.845	5.293%
β-Estradiol	3.456	13.870%
17-Ethinyl estradiol	1.889	27.915%
Estradiol-3-benzoate	1.472	−5.447%
Prednisolone	3.173	3.849%
Estriol	2.894	6.695%
Cholesterol	1.627	−1.571%
Cholic acid	3.186	11.922%
Norharmane	3.599	0.875%
Albendazole	3.556	−7.665%
MEABZ	3.525	−8.761%
Thiabendazole	3.488	−5.274%
Fuberidazole	3.424	8.400%
Allopurinol	3.571	−9.477%
6-Benzyladenine	3.357	−8.210%
Camptothecin	2.275	−12.556%
10-Hydroxycamptothecine	2.965	−4.800%
Kinetin	3.732	4.223%
TPP	2.934	6.183%
TPPZn	2.768	4.267%
TFP	3.266	10.118%
Clofazimine	2.606	−14.150%
Cinnarizine	3.971	−4.008%
Coumarin 6	2.518	−2.181%
Zaltoprofen	2.465	2.501%
VB_9	3.469	7.772%
VB_2	2.938	−1.164%
Guanine	2.459	−10.008%
2-Hydroxychalcone	3.131	−3.878%
Triamterene	3.188	−10.475%
Gefitinib	3.683	2.623%

dimensionless, which reflects their influence on log S, and the order is as follows: $A_3 > E_{3LUMO} > I_3 > \chi_1 > \log p_{1w}$.

Table 4 also showed that the values of the inflation factor VIF are all less than 10, indicating that each parameter is relatively independent and there is no collinearity problem. In addition, the statistical ${Q_{F1}}^2$, ${Q_{F3}}^2$ and CCC are 0.710, 0.890 and 0.863, respectively, in accordance to the eqn (10)–(12). This confirmed the good external predictive ability of the LSER-based model. The results show the proposed model could be employed to predict the solubilizing effect of cucurbit[7]uril for other drugs.

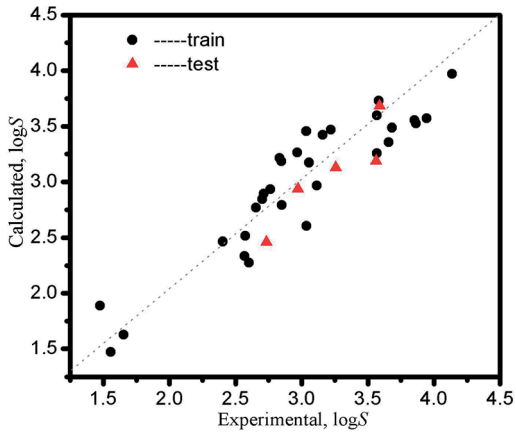

Fig. 3 The plot of calculated solubility values from the LSER-based model *vs.* the experimental solubility values.

The calculated log S data obtained from eqn (13) and the relative error are listed in Table 5, and the RE ($|\log S_{calculation} - \log S_{experimental}|/\log S_{experimental}$) are closed to 0.000. Fig. 3 indicates the LSER-based model is highly matched with the experimental values, where the data points are on both sides of the diagonal line and are close to the line. The dots represent the data points in the training set, and the triangles represent the data points in the test set.

3.2 Applicability domain

Applicability domain (AD) is defined to prove that the model has a satisfactory accuracy. The standardized residual (δ^*) is an important criterion, within the ±3 times the standards deviation (±3δ).[50] In addition to standardized residuals in the AD, leverage (h_i) is a common metric to evaluate the model accuracy.

$$\delta^* = \frac{y_i - \tilde{y}_i}{\sqrt{\sum_{i=1}^{n}(y_i - \tilde{y}_i)^2 \Big/ (n_{TR} - m - 1)}} \tag{14}$$

$$h_i = x_i^T (X^T X)^{-1} x_i \tag{15}$$

$$h_* = 3(m + 1)/n_{TR} \tag{16}$$

where x_i is column vector of the i-th drug parameter; X is 30 × 5 matrix of training set parameters; m is considered to be the number of descriptors (here $m = 5$); n_{TR} is the number of drugs in the training set (here $n_{TR} = 30$); h_* defines a warning value for leverage. Therefore, the warning value h_* of the LSER-based model (eqn (13)) is equal to 0.600. Fig. 4 shows that the standardized residuals of all drugs are in the acceptable range of (±3δ) and the leverage of all drugs is located within the defined AD. From the results, the proposed LSER-based model shows acceptable AD ranges.

3.3 Parameter analysis and interpretation

According to the proposed LSER model, solubilizing mechanism of cucurbit[7]uril could be explored.

 This journal is © The Royal Society of Chemistry 2020

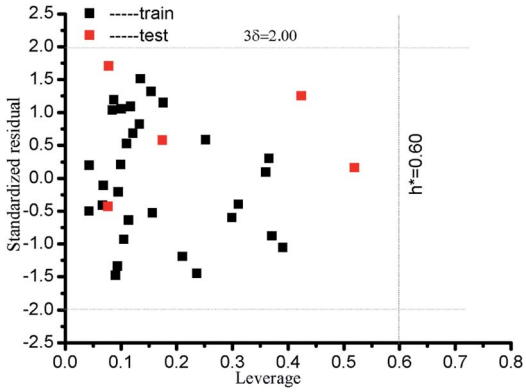

Fig. 4 Presentation of AD for all drugs by the LSER-based model using a Williams plot. The leverage (h_*) and standardized residual (δ^*) are shown by dashed lines on the x-axis and y-axis, respectively.

(a) The coefficient of the surface area of inclusion complexes is $a_3 = 22.859$, where the parameter A_3 has a positive correlation with log S. It indicates that the large surface area of inclusion complexes would promote the interaction between inclusion complexes and water solvent. Thus the solubility of inclusion complexes increases.

(b) The coefficient of the LUMO energy of inclusion complexes is $g_3 = 2.898$, where the parameter $E_{3\mathrm{LUMO}}$ has a positive correlation with log S. The LUMO energy indicates the ability of a molecule to accept electron pairs from neighbouring molecule. With larger LUMO energy, inclusion complexes could be easier to form hydrogen bonds with water, which enhances the solubility of inclusion complexes.

(c) The coefficient of the polarity index of inclusion complexes is $m_3 = 20.347$, where the parameter I_3 has a positive correlation with log S. When the polarity index is larger, the interaction with polar water molecules would be stronger. Then the solubility of inclusion complexes increases.

(d) The coefficient of the electronegativity of drugs $\chi_1 = 14.301$, where the parameter χ_1 has a positive effect with log S. According to the HOMO/LUMO orbital electron distribution diagram of inclusion complexes, it is known that LUMO is distributed on cucurbit[7]uril. If the drugs possess stronger electronegativity, it would be easier to form hydrogen bonds between the drugs and cucurbit[7]uril. Thus it increases the possibility for drugs entering the cavity of cucurbit[7]uril.

(e) The coefficient of the drug oil–water partition coefficient $p_{1\mathrm{w}} = -1.119$, where the parameter log $p_{1\mathrm{w}}$ has a negative correlation with log S. The oil–water partition coefficient mainly reflects the hydrophobic of drugs. This shows that the more hydrophobic the drug is, the stronger the repelling interaction will be in the mixed system. Then it is harder to dissolve in water and the solubility of drug decreases.

Table 6 The calculated log S data obtained from eqn (13) and the experimental solubility data

	log S_{Cal}	log S_{Exp}	RE
Cucurbit[8]uril	3.973	4.630	16.533%
Cucurbit[7]uril	3.863	3.525	−8.761%
Cucurbit[6]uril	3.380	1.450	−57.117%

Based on the above analysis, it is concluded that the surface area of inclusion complexes (A_3), the LUMO energy of inclusion complexes ($E_{3\mathrm{LUMO}}$), the polarity index of inclusion complexes (I_3), the electronegativity of drugs (χ_1), and the oil–water partition coefficient of drugs (log $p_{1\mathrm{w}}$) significantly affect the solubility of drugs by inclusions with cucurbit[7]uril.

3.4 Test on other macrocycles

As reported, for MEABZ the highest solubilities was obtained with cucurbit[6]uril (2.4 mM or 0.7 g L^{-1}), cucurbit[7]uril (7.3 mM or 2.3 g L^{-1}) and cucurbit[8]uril (9.4 mM or 2.9 g L^{-1}).[17] Although the model was developed for predicting the solubilizing property of cucurbit[7]uril, this work is mainly to build a model suitable for inclusion system. So to show the generality of the proposed model, the utilized parameters in LSER model were used to check the solubility of other macrocycles. According to Table 6, it could be found that the solubility of MEABZ with cucurbit[8]uril calculated from eqn (13) is close to the experimental solubility, and the overall trend is in accordance to the data reported in the literature. Thus it is possible to use this model for other macrocycles, such as cucurbit[8]uril or cucurbit[6]uril.

4. Conclusions

In this study, we proposed a LSER-based model by analysing different sorts of molecular parameters combined with the experimental solubility data of 35 drugs by inclusion with cucurbit[7]uril. The reported data of 30 drugs are applied as the training sets, while the rest data of 5 drugs are used as the test sets. Results show that the proposed model has good fitting and prediction ability. The model suggests that the solubility of inclusion complexes is not only dependent on the interaction between the inclusion complexes and the solvent, but also related to the interaction between the host and the guest. It further clarifies the surface area of inclusion complexes (A_3), the LUMO energy of inclusion complexes ($E_{3\mathrm{LUMO}}$), the polarity index of inclusion complexes (I_3), the electronegativity of drugs (χ_1), and the oil–water partition coefficient of drugs (log $p_{1\mathrm{w}}$) are effective parameters on log S. The influence of each parameter on log S is as follows: $A_3 > E_{3\mathrm{LUMO}} > I_3 > \chi_1 > \log p_{1\mathrm{w}}$. These parameters could be applied to calculate the solubilizing effect of other drugs by inclusion with cucurbit[7]uril or other macrocycles.

Conflicts of interest

There are no conflicts to declare.

Acknowledgements

The authors gratefully acknowledge financial support from the National Natural Science Foundation of China (NSFC grant number 21476186 and 21903066).

Notes and references

1 D. Ma, G. Hettiarachchi, D. Nguyen, B. Zhang, J. B. Wittenberg, P. Y. Zavalij, V. Briken and L. Isaacs, *Nat. Chem.*, 2012, **4**, 503–510.
2 J. A. Plumb, B. Venugopal, R. Oun, N. Gomez-Roman, Y. Kawazoe, N. S. Venkataramanan and N. J. Wheate, *Metallomics*, 2012, **4**, 561–567.
3 V. V. Sursyakova, V. A. Levdansky and A. I. Rubaylo, *Electrophoresis*, 2019, **40**, 1656–1661.
4 V. J. Stella and R. A. Rajewski, *Int. J. Pharm.*, 2020, **583**, 119396.
5 L. Wang, J. Yan, Y. Li, K. Xu, S. Li, P. Tang and H. Li, *J. Pharm. Biomed. Anal.*, 2016, **117**, 453–463.
6 C. Zhu, Z. H. Meng, W. L. Liu, H. W. Ma, J. R. Li, T. T. Yang, Y. Liu, N. Liu and Z. B. Xu, *R. Soc. Open Sci.*, 2018, **5**, 180038.
7 X. J. Loh, *Mater. Horiz.*, 2014, **1**, 185–195.
8 H. H. J. Buschmann, K. Jansen and E. Schollmeyer, *Inorg. Chem. Commun.*, 2003, **6**, 531–534.
9 D. Das, K. I. Assaf and W. M. Nau, *Front. Chem.*, 2019, **7**, 619.
10 B. Zhang and L. Isaacs, *J. Med. Chem.*, 2014, **57**, 9554–9563.
11 A. I. Lazar, F. Biedermann, K. R. Mustafina, K. I. Assaf, A. Hennig and W. M. Nau, *J. Am. Chem. Soc.*, 2016, **138**, 13022–13029.
12 B. U. Emenike, S. N. Bey, B. C. Bigelow and S. V. S. Chakravartula, *Chem. Sci.*, 2016, **7**, 1401–1407.
13 S. Yousefinejad, F. Honarasa, M. Mosahebfard and M. Nekoeinia, *J. Mol. Liq.*, 2017, **231**, 263–271.
14 P. W. Kenny, C. A. Montanari, I. M. Prokopczyk, J. F. Ribeiro and G. R. Sartori, *J. Med. Chem.*, 2016, **59**, 4278–4288.
15 E. L. Robinson, P. Y. Zavalij and L. Isaacs, *Supramol. Chem.*, 2014, **27**, 288–297.
16 S. M. Wang, J. M. Chen and T. B. Lu, CN 105641713A, 2016.
17 Y. Zhao, M. H. Pourgholami, D. L. Morris, J. G. Collins and A. I. Day, *Org. Biomol. Chem.*, 2010, **8**, 3328–3337.
18 Q. Liu, Q. Tang, Y.-Y. Xi, Y. Huang, X. Xiao, Z. Tao, S.-F. Xue, Q.-J. Zhu, J.-X. Zhang and G. Wei, *Supramol. Chem.*, 2015, **27**, 386–392.
19 H. Zhang, Y. Huang, S.-F. Xue, Z. Tao and Q.-J. Zhu, *Supramol. Chem.*, 2011, **23**, 527–532.
20 Y. Huang, S.-F. Xue, Z. Tao, Q.-J. Zhu, H. Zhang, J.-X. Lin and D.-H. Yu, *J. Inclusion Phenom. Macrocyclic Chem.*, 2008, **61**, 171–177.
21 F. Chandra, P. Kumar and A. L. Koner, *Colloids Surf., B*, 2018, **171**, 530–537.
22 G. Guo, Q. Tang, Y. Huang, Z. Tao, S. Xue and Q. Zhu, *Chin. J. Org. Chem.*, 2014, **34**, 2317.
23 Y. Lv, L. F. Yan and N. Dong, *Spectrosc. Spectral Anal.*, 2014, **34**, 1610–1614.
24 S. Li, J. Y.-W. Chan, Y. Li, D. Bardelang, J. Zheng, W. W. Yew, D. P.-C. Chan, S. M. Y. Lee and R. Wang, *Org. Biomol. Chem.*, 2016, **14**, 7563–7569.
25 R. H. Alzard, M. S. Bufaroosha, N. Al-Shamsi, A. Sohail, N. Al-Dubaili, A. A. Salem, I. M. Abdou and N. Saleh, *ACS Omega*, 2019, **4**, 953–960.
26 X. L. Li, Master thesis, Xi'an University of Architecture and Technology, 2014.
27 N. Barooah, J. Mohanty, H. Pal and A. C. Bhasikuttan, *J. Phys. Chem. B*, 2012, **116**, 3683–3689.
28 S. Li, X. Lin, K. Xu, J. He, H. Yang and H. Li, *Sci. Rep.*, 2017, **7**, 45984.
29 Z. Yang, D. Shao and G. Zhou, *J. Chem. Thermodyn.*, 2019, **132**, 268–275.
30 K.-U. Goss, *Fluid Phase Equilib.*, 2005, **233**, 19–22.
31 C. A. Baldasare and P. G. Seybold, *J. Phys. Chem. A*, 2020, **124**, 2152–2159.
32 T.-J. Park, Y. S. Kim, E. Kan and S. H. Lee, *RSC Adv.*, 2015, **5**, 25590–25593.
33 R. E. Skyner, J. L. McDonagh, C. R. Groom, T. van Mourik and J. B. Mitchell, *Phys. Chem. Chem. Phys.*, 2015, **17**, 6174–6191.
34 H. Liu, M. Wei, X. Yang, C. Yin and X. He, *Sci. Total Environ.*, 2017, **574**, 1371–1378.
35 G.-Y. Yang, J. Yu, Z.-Y. Wang, X.-L. Zeng and X.-H. Ju, *QSAR Comb. Sci.*, 2007, **26**, 352–357.
36 J. Huang, G. Yu, Z.-L. Zhang, Y.-L. Wang, W.-H. Zhu and G.-S. Wu, *J. Environ. Sci.*, 2004, **16**, 21–29.
37 J.-W. Chen, L. Feng, Y.-Y. Liao, S.-K. Han, L.-S. Wang and H.-M. Hu, *Chemosphere*, 1996, **33**, 537–546.
38 T. N. Borhani, S. Garcia-Munoz, C. Vanesa Luciani, A. Galindo and C. S. Adjiman, *Phys. Chem. Chem. Phys.*, 2019, **21**, 13706–13720.
39 Y. J. Jeon, S. Y. Kim, Y. H. Ko, S. Sakamoto, K. Yamaguchi and K. Kim, *Org. Biomol. Chem.*, 2005, **3**, 2122–2125.
40 B. Mennucci, *Wiley Interdiscip. Rev.: Comput. Mol. Sci.*, 2012, **2**, 386–404.
41 M. Agrawal, A. Kumar and A. Gupta, *RSC Adv.*, 2017, **7**, 41573–41584.
42 H. Szatyłowicz, *J. Phys. Org. Chem.*, 2008, **21**, 897–914.
43 C.-G. Zhan, J. A. Nichols and D. A. Dixon, *J. Chem. Phys.*, 2003, **107**, 4184–4195.
44 T. Lu and F. W. Chen, *J. Comput. Chem.*, 2012, **33**, 580–592.
45 L. T. Qin, X. Zhang, Y. H. Chen, L. Y. Mo, H. H. Zeng, Y. P. Liang, H. Lin and D. Q. Wang, *Environ. Sci. Pollut. Res. Int.*, 2019, **26**, 16606–16615.
46 Q. Xu, C. Wei, R. Liu, S. Gu and J. Xu, *Chemom. Intell. Lab. Syst.*, 2015, **146**, 313–321.
47 N. Chirico and P. Gramatica, *J. Chem. Inf. Model.*, 2011, **51**, 2320–2335.
48 L. Eriksson, J. Jaworska, A. P. Worth, M. T. Cronin, R. M. McDowell and P. Gramatica, *Environ. Health Perspect.*, 2003, **111**, 1361–1375.
49 J. G. Topliss and R. P. EdwardsJ, *J. Med. Chem.*, 1979, **22**, 1239–1244.
50 S. Yousefinejad, F. Honarasa and H. Montaseri, *RSC Adv.*, 2015, **5**, 42266–42275.

 This journal is © The Royal Society of Chemistry 2020